

1 Early Silurian $\delta^{13}\text{C}_{\text{org}}$ excursions in the foreland basin of Baltica, both familiar
2 and surprising

3

4 Emma U. Hammarlund^{1,2*}, David K. Loydell³, Arne T. Nielsen⁴, and Niels H. Schovsbo⁵

5

6 Affiliations:

7 ¹Translational Cancer Research, Laboratory Medicine, Lund University, Medicon Village

8 404:C3, Scheelevägen 2, 223 63 Lund, Sweden.

9 ²Nordic Center for Earth Evolution, University of Southern Denmark, Campusvej 55, 5230

10 Odense M, Denmark.

11 ³School of Earth and Environmental Sciences, University of Portsmouth, Burnaby Road,

12 Portsmouth PO1 3QL, United Kingdom.

13 ⁴Department of Geosciences and Natural Resource Management, University of Copenhagen,

14 Øster Voldgade 10, 1350 København K, Denmark.

15 ⁵Geological Survey of Denmark and Greenland, Øster Voldgade 10, DK-1350 Copenhagen K,

16 Denmark.

17

18 *Corresponding author e-mail: emma.hammarlund@med.lu.se

19

20

21 Abstract

22 The Sommerodde-1 core from Bornholm, Denmark, provides a nearly continuous
23 sedimentary archive from the Upper Ordovician through to the Wenlock Series (lower Silurian),
24 as constrained by graptolite biostratigraphy. The cored mudstones represent a deep marine
25 depositional setting in the foreland basin fringing Baltica and we present high-resolution data
26 on the isotopic composition of the section's organic carbon ($\delta^{13}\text{C}_{\text{org}}$). This chemostratigraphical
27 record is correlated with previously recognized $\delta^{13}\text{C}$ excursions in the Upper Ordovician–lower
28 Silurian, including the Hirnantian positive isotope carbon excursion (HICE), the early Aeronian
29 positive carbon isotope excursion (EACIE), and the early Sheinwoodian positive carbon isotope
30 excursion (ESCIE). A new positive excursion of high magnitude ($\sim 4\%$) is discovered in the
31 Telychian *Oktavites spiralis* Biozone (lower Silurian) and we name it the Sommerodde Carbon
32 Isotope Excursion (SOCIE). The SOCIE appears discernible in $\delta^{13}\text{C}_{\text{carb}}$ data from Latvian and
33 Estonian cores but it is not yet widely recognized. However, the magnitude of the excursion
34 within the deep, marine, depositional setting, represented by the Sommerodde-1 core, suggests
35 that the SOCIE reflects a significant event. In addition, the chemostratigraphical record of the
36 Sommerodde-1 core reveals the negative excursion at the transition from the Aeronian to
37 Telychian stages (the 'Rumba low'), and suggests that the commencement of the EACIE at the
38 base of the *Demirastrites triangulatus* Biozone potentially is a useful chemostratigraphical
39 marker for the base of the Aeronian Stage.

40

41 Keywords

42 Chemostratigraphy, Sommerodde-1 core, SOCIE, *Oktavites spiralis* Biozone, $\delta^{13}\text{C}_{\text{org}}$, Rumba
43 low

44

45 1 Introduction

46 Climate changes that affected and directed the course of early animal evolution were
47 perhaps never more dramatic than during the Ordovician and Silurian periods, as indicated by
48 evidence of recurring glacial deposits, sea-level changes, biotic turnover, and perturbations of
49 the global carbon cycle (Calner, 2008; Díaz-Martínez and Grahn, 2007; Harper et al., 2014;
50 Loydell, 2007; Melchin and Holmden, 2006; Servais et al., 2009). While changes in glacial
51 coverage, sea-level, and biology leave both physical and chemical evidence, perturbations in
52 the global carbon cycle are largely inferred from excursions in the isotopic composition of
53 sedimentary carbon (Veizer, 2005). For example, our understanding of the isotopic excursions
54 in the Silurian has developed in large part from rocks preserved in the Baltic basin and, now, a
55 handful of discrete and geographically widespread positive excursions has been recognized
56 (Cramer et al., 2011). However, the detailed correlation of these events and whether they
57 accurately reflect changes in global biogeochemical conditions are ongoing debates. Indeed, it
58 is questioned whether the sedimentary $\delta^{13}\text{C}$ features record changes in open-ocean seawater or
59 changes in diagenetic regimes (e.g. Ahm et al., 2017; Fanton and Holmden, 2007). These
60 debates benefit from isotopic data that are well-constrained in terms of both biostratigraphy and
61 palaeodepositional depth.

62 Advances in graptolite biostratigraphy have facilitated the successful identification and
63 dating of fluctuations in the Silurian carbon isotope record. The widespread distribution of
64 Silurian graptolites has enabled the definition of distinct and useful graptolite biozones, and a
65 robust biostratigraphy is established (see e.g. Cramer et al., 2011; Koren' and Bjerreskov, 1997;
66 Loydell, 1998). However, uncertainties pertaining to the biostratigraphy still remain. For
67 example, the calibration of records between conodont-bearing and graptolite-bearing
68 successions is often challenging because conodonts generally inhabited shallower water and
69 graptolites generally deeper water. Only occasionally (e.g. Loydell, 1998; Loydell et al., 2003;
70 Loydell et al., 2010) are both groups found in sufficient abundance and diversity within a single

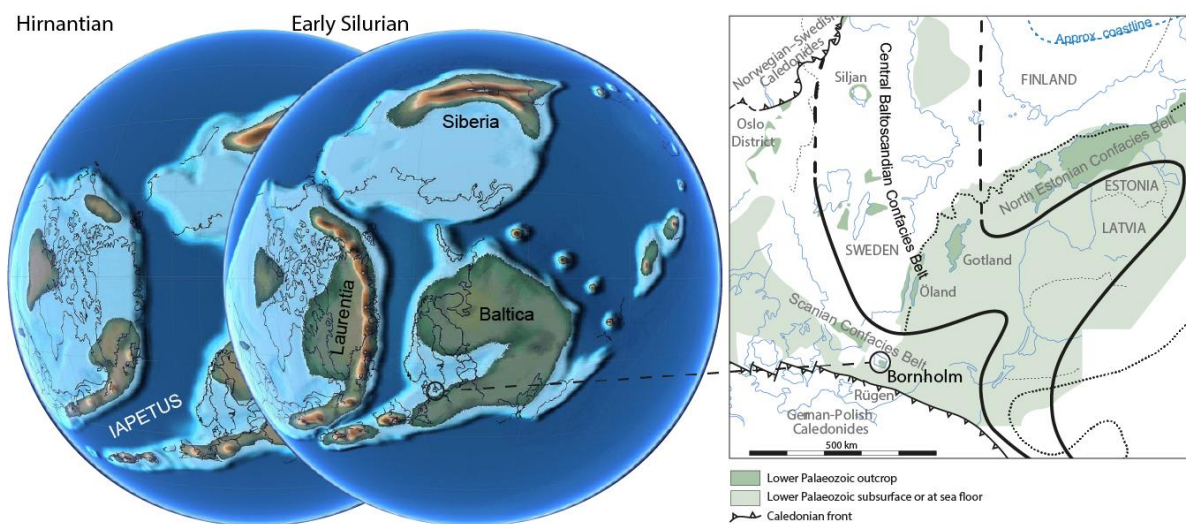
71 section to enable integration of the conodont and graptolite biozonations. Studies of
72 biostratigraphically well-constrained Silurian successions are thus essential in order to improve
73 interpretations of the $\delta^{13}\text{C}$ record.

74 Depositional depth appears to influence trends in the $\delta^{13}\text{C}$ record in ways that relate to
75 either the primary chemical conditions or diagenetic changes. For example, the magnitude of
76 Silurian global positive $\delta^{13}\text{C}$ excursions declines basin-ward for reasons yet unknown (Loydell,
77 2007). Processes in shallow settings appear to affect the amplification, alteration, and mixing
78 of $\delta^{13}\text{C}$ trends. For example, restricted circulation (Fanton and Holmden, 2007) or diagenesis
79 (Higgins et al., 2018) have specific impacts on the captured $\delta^{13}\text{C}$. Considering that separate
80 isotopic fingerprints may be mixed, especially in shallow settings, deep palaeodepositional sites
81 can provide a particularly valuable record. Outboard settings were also less directly affected by
82 eustatic sea-level changes that were common in the Ordovician and Silurian. Generally, the
83 major sea-level changes were associated with $\delta^{13}\text{C}$ excursions (Fanton and Holmden, 2007;
84 Holmden et al., 1998; Loydell, 2007). However, deep or outboard settings are underrepresented
85 in the rock record. Therefore, in order to decipher the causality between sea-level changes,
86 diagenesis, and $\delta^{13}\text{C}$ excursions, the deepest settings are essential since they appear to record
87 the most significant carbon isotope events that affected open marine conditions (Loydell, 2007).

88 Here we study the Sommerodde-1 core from Bornholm, Denmark, for which a graptolite
89 biozonation was established by Loydell et al. (2017). The depositional site represents
90 hemipelagic sedimentation in a deep foreland basin that was connected to the Iapetus Ocean
91 and, thus, to the global ocean (Koren' and Bjerreskov, 1997). Our study focuses on the $\delta^{13}\text{C}_{\text{org}}$
92 record from the uppermost Ordovician (Hirnantian) to the Wenlock in the Silurian. In addition
93 to several familiar carbon excursions described from other sections, the work demonstrates the
94 presence of a previously unrecognized and significant positive carbon excursion in the
95 Telychian *Oktavites spiralis* Biozone.

96 2 Geological setting

97 Baltica was located at equatorial latitudes during the Silurian and large parts of the craton
98 were flooded by a shallow epicontinental sea. However, the craton was on a collisional path
99 with Laurentia and Avalonia, as the separating Tornquist Sea and Iapetus Ocean narrowed and
100 eventually disappeared. In the process, peripheral foreland basins were established along the
101 western and southern margins of Baltica and rather great thicknesses of sediment were
102 deposited. Eventually, these foreland basins disappeared during the Caledonian Orogeny in the
103 later parts of the Silurian and concomitantly, the Baltic epicontinental sea became increasingly
104 restricted (Figure 1).



105
106 Figure 1. Palaeogeographical reconstruction showing the position of Baltica from the Late Ordovician
107 (Hirnantian) to the early Silurian (Scotese, 2001 and personal communication), and the distribution of
108 Lower Paleozoic strata in Scandinavia (modified from Calner et al., 2013; Nielsen, 2004; Stouge, 2004).

109 In the early Silurian, however, a foreland basin was still covering southernmost
110 Scandinavia. The Silurian succession preserved in onshore Bornholm – documented almost in
111 its entirety by the studied Sommerodde-1 core – is presumed to have been deposited in the
112 deeper parts of this foreland basin. Depositional depth may have been $\sim 1000 \pm 300$ m according
113 to Bjerreskov and Jørgensen (1983), a figure based on calculations of the settling conditions of

114 volcanic ash. In the area from south Sweden to north Germany (Scania–Bornholm–Rügen), the
115 thickness of individual biozones can vary substantially as the depositional centre in the foreland
116 basin progressively migrated northwards during the Silurian (Loydell et al., 2017; Maletz,
117 1997). The Silurian succession on Bornholm, 170 m thick in the Sommerodde-1 core, is
118 strongly dominated by mudstones but contains common diagenetic limestone in some intervals
119 (Bjerreskov, 1975; Koren' and Bjerreskov, 1997; Schovsbo et al., 2016). The basin appears to
120 have been fairly open during the studied time interval, which is evidenced by the presence of
121 geographically widespread graptolites (recognized e.g. in the studied core) and conodont taxa
122 (recognized e.g. on Gotland) (Cramer et al., 2011 and references therein).

123 Traditionally, the Silurian shales on Bornholm have been assigned to the Rastrites and
124 *Cyrtograptus* shales, but there is no well-defined boundary between these units; overall the
125 Rastrites shale tends to be darker grey and the *Cyrtograptus* shale tends to be lighter grey. The
126 stratigraphy of the Silurian shales in onshore Bornholm has been discussed by Bjerreskov
127 (1975), Koren' and Bjerreskov (1997), and Loydell et al. (2017); for older references, see these
128 papers. The investigated succession straddles the Hirnantian (Upper Ordovician) through the
129 Rhuddanian, Aeronian, Telychian and Sheinwoodian (all lower Silurian). The succession was
130 deeply buried in the late Silurian–Early Devonian and the thermal maturity is about 2.3 % R_0
131 (Petersen et al., 2013).

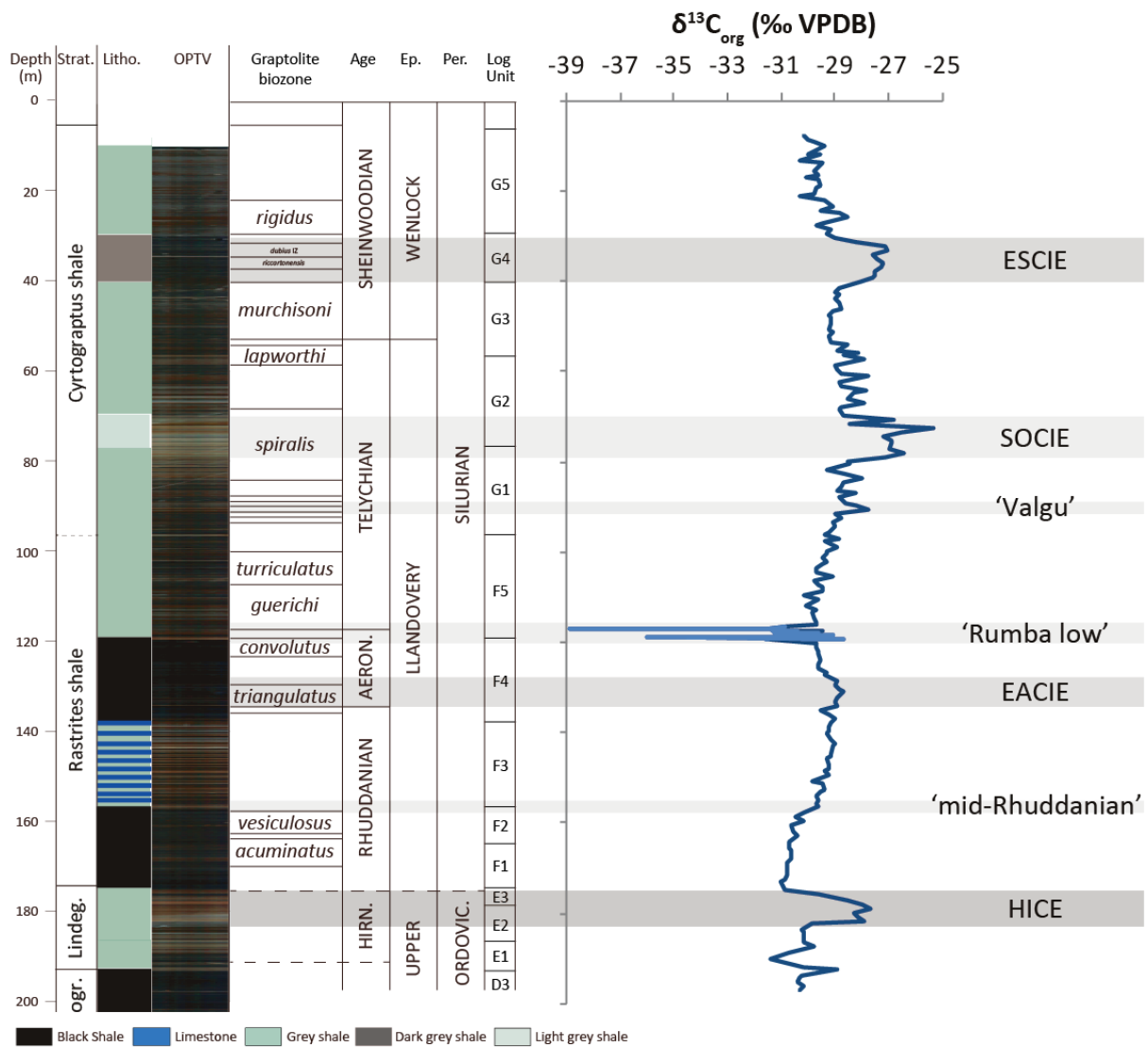
132 3 Material and methods

133 The core interval 7.5–197.2 m in the Sommerodde-1 core (DGU 248.62), southern
134 Bornholm, was sampled with an average spacing of 0.78 m; for details of the location of the
135 drill site, see Loydell et al. (2017). The samples were crushed at GEUS in an agate swing mill
136 to below 250 micrometres. Isotope analyses of organic carbon were performed at the Nordic
137 Center for Earth Evolution, University of Southern Denmark, by isotope ratio mass

138 spectrometry (Thermo Delta V plus) after combustion in an elemental analyser Flash EA 2000.
139 For calibration of C isotope determinations, international standards of sediment (IVA 33802151
140 with $\delta^{13}\text{C}_{\text{VPDB}}$ -26.07 ‰), protein (IVA 33802155 with $\delta^{13}\text{C}_{\text{VPDB}}$ -26.98 ‰), and urea (IVA
141 33802174 with $\delta^{13}\text{C}_{\text{VPDB}}$ -45.38 ‰) were used. The isotopic composition of carbon ($\delta^{13}\text{C}$) is
142 reported as relative to the Vienna Pee Dee Belemnite (VPDB), with a precision of 0.1 ‰. The
143 data is reported in Figures 3-7 where the scale varies ($\delta^{13}\text{C}_{\text{VPDB}}$) but vertical gridlines are set at
144 a distance of 2 ‰.

145 4 Results

146 A total of 297 new $\delta^{13}\text{C}_{\text{org}}$ data points was generated for this study (Appendix A). The
147 analyzed samples derive from an interval straddling the Hirnantian (Upper Ordovician) to the
148 Sheinwoodian (lower Silurian) and the data are shown in Figure 2. Samples from the
149 Sommerodde-1 core have a mean of -29.4 ‰ and a standard deviation of 1.25 ‰. Values
150 significantly higher (+1 s.d.) than the average (over -28.2 ‰) are found in the Hirnantian, the
151 Telychian, and the Sheinwoodian, while significantly lower (-1 s.d.) values (below -30.7 ‰)
152 are found at the transition between the Aeronian and the Telychian (see grey shadings in Figure
153 2). Additionally, a modest positive excursion of ~ 1 ‰ $\delta^{13}\text{C}_{\text{org}}$ values compared to values in
154 samples immediately below and above, is recognized in the lower Aeronian and a small positive
155 shift is seen in the middle Rhuddanian. The results are further presented in Figures 3–7 and
156 discussed in detail below.



157

158 Figure 2. A log of the Sommerrode-1 well with depth, stratigraphy (strat.), lithology (litho.), optic
 159 televiewer (OPTV), graptolite biozones, Age, Epoch (Ep), Period (Per), log units, and the $\delta^{13}C_{org}$ data
 160 through the succession. Shaded bands highlight features in the data that we discuss: three are previously
 161 recognized excursions (dark grey) – the Hirnantian isotopic carbon excursion (HICE), the early
 162 Aeronian carbon isotope excursion (EACIE) and the early Sheinwoodian carbon isotope excursion
 163 (ESCIE). Other excursions (light grey bands) are new, negative or less well-recognized. For the ‘mid-
 164 Rhuddanian’ excursion only the onset of the excursion is shaded. For values in the interval with high-
 165 resolution sampling (light blue line), see SI data. Scale ranges from -25 to -39 ‰. Lithology, OPTV,
 166 and log units from Schovsbo et al. (2015) and biozones from Loydell et al. (2017).

167

168 5 Discussion

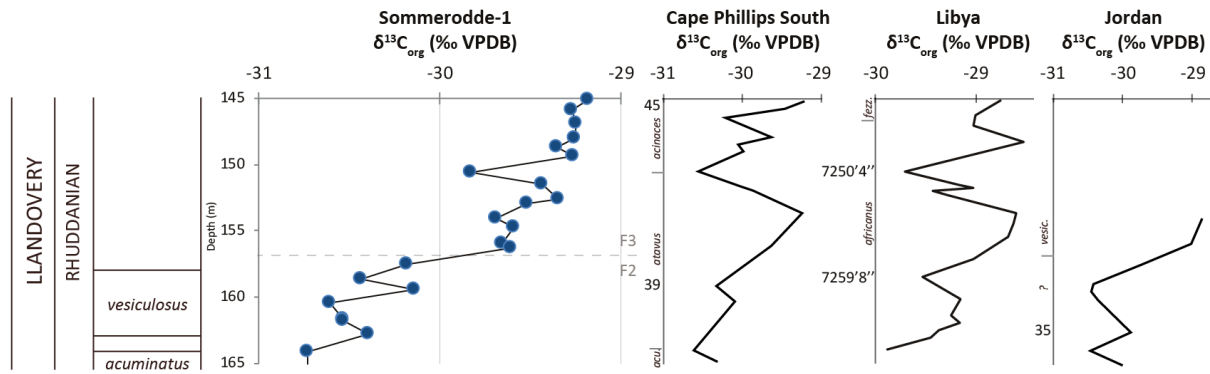
169 The following features can be recognized in the $\delta^{13}\text{C}_{\text{org}}$ record measured in the
170 Sommerodde-1 core, discussed in ascending order. We define an excursion to range between
171 the first and last sample that has higher $\delta^{13}\text{C}_{\text{org}}$ values than baseline values of that interval.

172 5.1 The HICE

173 The Hirnantian positive isotope carbon excursion (HICE), observed globally, is
174 recognized in the Sommerodde-1 core in the interval from 182.47 m to 175.96 m (Figure 2).
175 This interval comprises most of the Lindegård Formation, which, in another core from
176 Bornholm (Billegrav-2), has been determined to belong to the *Metabolograptus persculptus*
177 Biozone in the Upper Ordovician Hirnantian Stage (Hammarlund et al., 2012). In the
178 Sommerodde-1 core, the HICE has an amplitude of ~ 3 ‰.

179 5.2 The mid-Rhuddanian positive shift in $\delta^{13}\text{C}_{\text{org}}$

180 The Sommerodde-1 data exhibit a small, positive shift in $\delta^{13}\text{C}_{\text{org}}$ values at the transition
181 between log units F2 and F3 at 156.9 m (Figure 3). No distinct excursion is discernible and the
182 shift is small. However, the very distinctive alternating dark grey and pale grey carbonate
183 cemented mudstones of log unit F3 (Loydell et al., 2017, fig 3) were shown by Koren' and
184 Bjerreskov (1997) to have their base within the lower part of the *Cystograptus vesiculosus*
185 Biozone in which a positive excursion is observed elsewhere (e.g. Melchin and Holmden,
186 2006). A minor shift is observed in the deep-water successions of Dob's Linn, Scotland
187 (Underwood et al., 1997) and at Cape Phillips South on Anticosti Island in Canada (Melchin
188 and Holmden, 2006). Correspondingly, a minor positive $\delta^{13}\text{C}_{\text{org}}$ excursion of mid-Rhuddanian
189 age is recognized in the E1-NC174 core of the Murzuq Basin in Libya (Loydell et al., 2013).
190 Also, the rising limb of what is considered to be the same excursion is present in the BG-14
191 core from southern Jordan (Armstrong et al., 2009; Armstrong et al., 2005; Loydell et al., 2009).



192

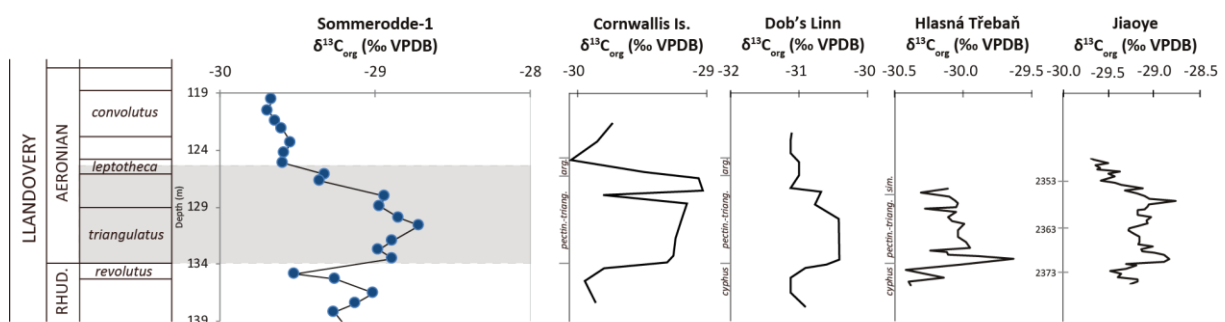
193 Figure 3. The onset of the positive carbon isotope excursion in the mid-Rhuddanian in the Sommerrodde-
 194 1 core (this study), correlated to carbon isotope data described in the section at Cape Phillips South in
 195 Canada (Melchin and Holmden, 2006), the Libyan core E1-NC174 (Loydell et al., 2013) and in the
 196 Jordanian core BG-14 (Loydell et al., 2009). Scale for the Sommerrodde-1 data ranges from -29 to -31
 197 ‰. For log units (F2-F3), see Schovsbo et al 2015 and Figure 2.

198 The correlation between these areas relies on detailed graptolite biostratigraphy, to which
 199 we can relate the Sommerrodde-1 data. The Libyan core (E1-NC174) contains a largely endemic
 200 graptolite fauna (Loydell, 2012), whereas the Jordanian core (BG-14) yielded a mixture of
 201 North African and Arabian endemics as well as more widespread taxa that enabled application
 202 of the ‘standard’ graptolite biozonation by Loydell et al. (2009). In the Jordanian core, the minor
 203 positive shift in $\delta^{13}\text{C}_{\text{org}}$ values occurs in strata lacking diagnostic graptolites but that overlie
 204 beds containing an upper *Akidograptus ascensus*-*Parakidograptus acuminatus* Biozone
 205 assemblage and underlie beds containing a *Cystograptus vesiculosus* Biozone graptolite
 206 assemblage. In the lowest assemblage assignable to the *C. vesiculosus* Biozone in the Jordanian
 207 BG-14 core (at a depth of 30.0 m), *Dimorphograptus confertus* is present. However, *D.*
 208 *confertus* occurs in the middle and upper parts of the *C. vesiculosus* Biozone elsewhere (Koren’
 209 and Bjerreskov, 1997; Štorch, 1994a). Thus, the presence of *D. confertus* in immediately
 210 overlying strata strongly suggests that the rise in $\delta^{13}\text{C}_{\text{org}}$ values (between 30.9 m and 30.0 m in
 211 the BG-14 core) is within the *C. vesiculosus* Biozone.

212 Taken together, it seems likely that the positive $\delta^{13}\text{C}_{\text{org}}$ shift seen between log units F2 and
 213 F3 in the Sommerodde-1 core correlates with a similar shift seen in a handful of sections
 214 around the world, and that the onset of this minor excursion commenced in the lower part of
 215 the *C. vesiculosus* Biozone.

216 5.3 The early Aeronian positive excursion (EACIE)

217 In the Sommerodde-1 core, a positive $\delta^{13}\text{C}$ excursion of ~ 0.8 ‰ is observed at the
 218 transition from the Rhuddanian to the Aeronian between 133.93 m and 126.55 m (Figure 4).
 219 The excursion starts at the base of the *Demirastrites triangulatus* Biozone (at 133.93 m). The
 220 uppermost sample of the excursion (at 126.55 m) is from an interval lacking diagnostic index
 221 fossils, but which lies above the highest confidently assigned *Demirastrites triangulatus*
 222 Biozone sample (at 129.80 m) and below the lowest definite *Pribylograptus leptotheca* Biozone
 223 sample (at 126.75 m). Within this interval, the graptolite *Demirastrites pectinatus* occurs (in
 224 the 128.11–128.13 m sample), which has been shown recently to be restricted to the *D.*
 225 *pectinatus* and lowermost *Demirastrites simulans* biozones that overlie the *D. triangulatus*
 226 Biozone (Štorch et al., 2018). Hence, *D. pectinatus* constrains the end of the excursion to be
 227 somewhere within the *D. pectinatus* and lowermost *D. simulans* biozones.



228
 229 Figure 4. The positive early Aeronian carbon isotope excursion (EACIE) in the Sommerodde-1 core
 230 (this study), correlated to carbon isotope data described in the sections at Cornwallis Island in Canada
 231 (Melchin and Holmden, 2006), Dob's Linn in Scotland (Melchin and Holmden, 2006), Hlasná Třebaň

232 in the Czech Republic (Štorch et al., 2018), and in the Jiaoye core from the Yangtze platform, China
233 (Liu et al., 2017). Scale for the Sommerodde-1 data ranges from -28 to -32 ‰.

234 The EACIE is of small magnitude, but widely recognized, as shown first by Melchin and
235 Holmden (2006) and subsequently by others, e.g. Cramer et al. (2011) and Melchin et al.
236 (2012). The excursion is noted in at least two other deep-water successions, at Dob's Linn,
237 Scotland, and Cape Manning, Arctic Canada (Heath, 1998; Melchin and Holmden, 2006). The
238 $\delta^{13}\text{C}_{\text{carb}}$ and $\delta^{13}\text{C}_{\text{org}}$ data generally record the EACIE similarly, but not always (see e.g. Kaljo in
239 Põldvere, 2003, Martma in Põldvere 2003). In the Ruhnu (500) core from Estonia, a positive
240 excursion is present through the basal 20 m of the Aeronian Ikla Formation (Martma in
241 Põldvere, 2003), where the key taxon *Demirastrites triangulatus* occurs throughout (Kaljo in
242 Põldvere, 2003). However, in the Ikla core, also from Estonia, a positive $\delta^{13}\text{C}_{\text{carb}}$ shift in the
243 lowermost Aeronian coincides with a negative $\delta^{13}\text{C}_{\text{org}}$ excursion, see Gouldey et al. (2010) and
244 the graptolite stratigraphy from Kaljo and Vingisaar (1969). From a widely separate
245 palaeobasin, in the Jiaoye-1 core from the Yangtze platform in China, a minor positive $\delta^{13}\text{C}_{\text{org}}$
246 excursion is noted immediately *below* the base of the *D. triangulatus* Biozone in strata assigned
247 to the Rhuddanian (Liu et al., 2017, fig 7). However, this part of the Jiaoye-1 core is
248 biostratigraphically poorly documented. The excursion commences at 2370.2 m, but no
249 biostratigraphically useful graptolites were recorded in the interval 2378.97-2368.97 m and the
250 lowest Aeronian graptolite documented (*Rastrites longispinus* at 2368.97 m) is not known from
251 the lowermost part of the *D. triangulatus* Biozone (Štorch et al., 2018; Zalasiewicz et al., 2009).
252 Thus, it appears likely that the excursion in the Jiaoye-1 core commences within the basal
253 Aeronian, rather than in the upper Rhuddanian. Similarly, the commencement of the excursion
254 at Cape Manning, Canada, is poorly constrained where only overlying strata are
255 biostratigraphically assigned (to the *D. pectinatus* Biozone) (Melchin & Holmden 2006).
256 Hence, the onset of the excursion may indeed align with the base of the Aeronian, as elsewhere.

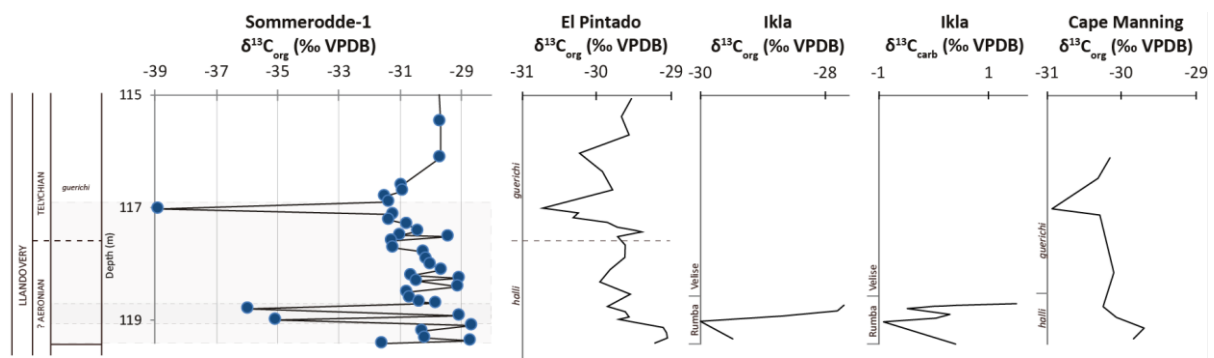
257 These examples emphasize the value of robust biostratigraphical markers for recognition of, at
258 least the commencement, of the EACIE.

259 The candidate GSSP section Hlasná Třebaň in the Czech Republic includes the EACIE (as
260 measured in $\delta^{13}\text{C}_{\text{org}}$) commencing at the very base of the *D. triangulatus* Biozone (Štorch et al.,
261 2018). Since the EACIE commences at an identical level also on Bornholm, the base of the *D.*
262 *triangulatus* Biozone (and Aeronian Stage) may have a very useful chemostratigraphical
263 marker.

264 5.4 The tentative presence of the *sedgwickii* Biozone excursion and the Rumba low

265 The significant positive excursion in the *S. sedgwickii* Biozone as observed at Dob's Linn,
266 Scotland (Melchin and Holmden, 2006), in Arctic Canada (Melchin and Holmden, 2006), Nova
267 Scotia, Canada (Melchin et al., 2014), and Bohemia (Štorch and Frýda, 2012) is not clearly
268 discernible in the Sommerodde-1 core. Indeed, initial analysis of the Sommerodde-1 core
269 samples, which were taken at approximately 1 m intervals, was complemented by more densely
270 spaced sampling (10 cm intervals) at this level. The complementary samples were taken through
271 the unfossiliferous grey silty mudstones of the lowermost part of log unit F5 (base at 119.4 m,
272 see Figure 2 and Schovsbo et al., 2015) that overlies the highly fossiliferous black mudstones
273 of the *Lituigraptus convolutus* Biozone (Aeronian), and up into an interval with graptolitic
274 horizons yielding *Spirograptus guerichi* Biozone taxa (Telychian) at 116.60 m. Three samples
275 have particularly positive values (-28.71 ‰, -28.66 ‰, and -29.07 ‰ occurring at 119.37 m,
276 119.08 m, and 118.92 m, respectively), in the range of peak values observed elsewhere during
277 the *S. sedgwickii* Biozone (Figure 5). The three positive values occur in a decreasing trend and
278 may be a manifestation of the falling limb, or at least part of, the *S. sedgwickii* Biozone
279 excursion (which in the stratigraphically expanded sequence on Nova Scotia, Canada (Melchin
280 et al., 2014), comprises several separate peaks). Although the presence of an excursion is
281 tentatively suggested, no major positive excursion is observed. The absence of a major

282 excursion suggests that the boundary between log units F4 and F5 is an unconformity (Figure
 283 2). The interpreted unconformity in the Sommerodde-1 core spans probably from the
 284 *Stimulograptus sedgwickii* Biozone and possibly also the overlying *Stimulograptus halli*
 285 Biozone (upper Aeronian) (cf. Loydell et al., 2017). These biozones are absent (or
 286 unfossiliferous) in the nearby Øleå section (Bjerreskov, 1975) and a thin conglomerate is
 287 developed at this level in the Billegrav-2 core (A.T. Nielsen unpublished; see Schovsbo et al.
 288 (2015) for location), suggestive of a stratigraphical break. Indeed, the *S. sedgwickii* Biozone is
 289 commonly absent in other sequences on Baltica (e.g. Loydell et al., 2010; Walasek et al., 2018).



290
 291 Figure 5. Particularly low values in the uppermost Aeronian and lowermost Telychian marked with pale
 292 grey boxes represent the ‘Rumba low’. Scale ranges from -28 to -39 ‰. The Sommerodde-1 data are
 293 correlated to carbon isotope data described from the El Pintado sections in Spain (Loydell et al., 2015),
 294 the Ikla core in Estonia (Gouldey et al., 2010; Kaljo and Martma, 2000), and the sections at Cape
 295 Manning in Canada (Melchin and Holmden, 2006). Dashed line marks the presumed boundary between
 296 the Aeronian and Telychian.

297 The densely sampled transition from the Aeronian to the Telychian (119.50 m to 116.60
 298 m) is characterized by generally low $\delta^{13}\text{C}$ values ($\sim 30.9 \text{ ‰} \pm 2.0$) (Figure 5). Also, in the lower
 299 Telychian strata of the Sommerodde-1 core, two remarkably low $\delta^{13}\text{C}_{\text{org}}$ values, -35.05 ‰ and
 300 -35.97 ‰, have been recorded at 119.0 m and 118.8 m, respectively. These two samples derive
 301 from the lower part of the unfossiliferous siltstone assigned to log unit F5 (Schovsbo et al.,
 302 2015). A single, even lower $\delta^{13}\text{C}_{\text{org}}$ value, -38.89 ‰, occurs at 117.01 m (Figure 5). A graptolite
 303 sample from 117.14–117.13 m yielded a lower *guerichi* Biozone assemblage comprising

304 *Streptograptus pseudoruncinatus*, ‘*Monograptus*’ *gemmatus*, and *Rastrites maximus* (Loydell
305 et al., 2017), which shows that the 117.01 m $\delta^{13}\text{C}_{\text{org}}$ sample is of earliest Telychian age. A
306 negative $\delta^{13}\text{C}$ excursion has been recorded close to the Aeronian–Telychian boundary in many
307 sections in the Baltic region and elsewhere, in both $\delta^{13}\text{C}_{\text{carb}}$ and $\delta^{13}\text{C}_{\text{org}}$ data (Gouldey et al.,
308 2010). This negative excursion is referred to as the “Rumba low”, named after the Rumba
309 Formation in Estonia (Kaljo and Martma, 2000). Walasek et al. (2018) discuss the age of the
310 Rumba low, noting that different authors refer to it as either late Aeronian (Kaljo and Martma,
311 2000), early Telychian (Gouldey et al., 2010), or straddling the Aeronian–Telychian boundary
312 (Cramer et al., 2011). In the Ikla core, Estonia, the lowest values occur in strata containing
313 *Metaclimacograptus hughesi* which is a common and widespread species that ranges to the very
314 top of the Aeronian (Loydell et al., 2015) but is not known to extend into the Telychian. Hence,
315 the presence of *Me. hughesi* strongly suggests a latest Aeronian age of the excursion in Estonia,
316 but in the El Pintado section, Spain, and at Cape Manning on Anticosti Island, Canada, the
317 lowest $\delta^{13}\text{C}_{\text{org}}$ values are demonstrably within the lower *guerichi* Biozone and thus of early
318 Telychian age (Loydell et al., 2015; Melchin and Holmden, 2006). The Sommerodde-1 core
319 provides additional evidence that the stratigraphically highest and very low $\delta^{13}\text{C}$ value
320 characterizing the Rumba low occurs in the lower Telychian, consistent with the Canadian and
321 El Pintado data. The other two samples with very low values at 119.0 and 118.8 m, i.e.
322 immediately above the unconformity, may theoretically be of latest Aeronian age, which would
323 be consistent with the Ikla core data but this remains uncertain. In any case, considering the
324 Estonian records, the Rumba low appears to straddle the Aeronian–Telychian boundary and
325 represents a useful chemostratigraphical marker for this chronostratigraphical boundary.

326 No cause has been proposed for the Rumba low as yet. In terms of global environmental
327 changes, the latest Aeronian–earliest Telychian is characterized by rapid sea-level rise (Loydell,
328 1998), with many localities at this time seeing deposition of graptolitic muds above

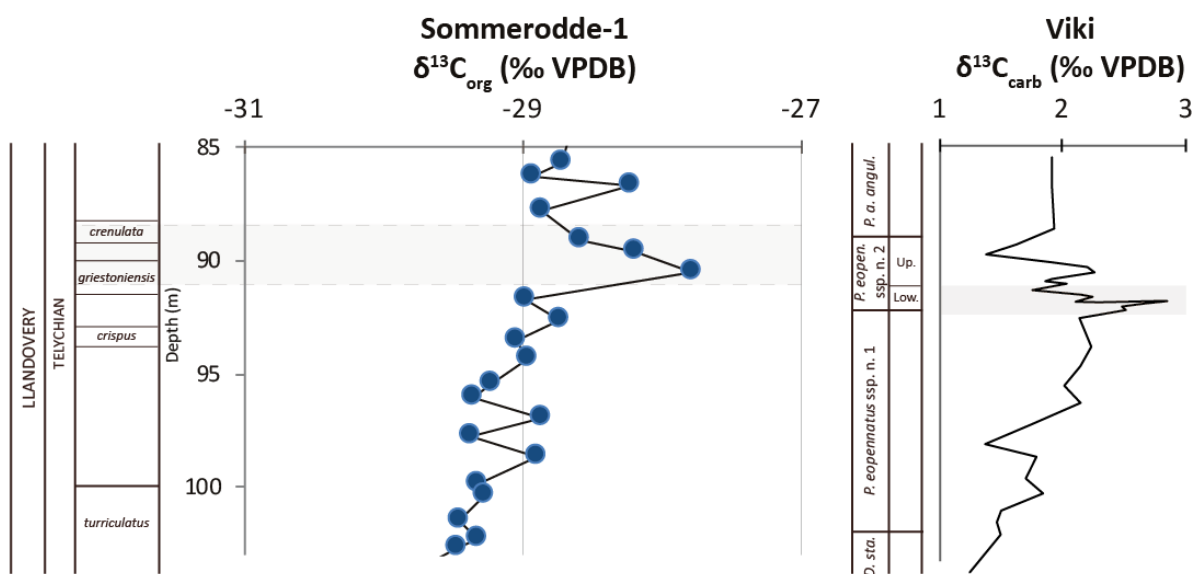
329 unconformities or shallower water sediments. In this respect, it is noteworthy that low $\delta^{13}\text{C}_{\text{org}}$
330 values occur both below and above the inferred unconformity in the Sommerodde-1 core. If the
331 unconformity represents an episode of low sea-level followed by a sea-level rise, it is
332 worthwhile considering whether the mode of early diagenesis may also have shifted. Depending
333 on whether early diagenesis is buffered by seawater (in deep or outboard settings with
334 hemipelagic sedimentation) or sediment (shallow depositional conditions or in the vicinity of
335 restricted platform settings), the isotopic composition may locally change by several permil
336 (plus or minus) in $\delta^{13}\text{C}_{\text{carb}}$ and, subsequently, $\delta^{13}\text{C}_{\text{org}}$ values (Ahm et al., 2018; Higgins et al.,
337 2018). A diagenetic influence could also be indicated by how both the $\delta^{13}\text{C}_{\text{org}}$ and $\delta^{13}\text{C}_{\text{carb}}$
338 records of platform settings synchronously demonstrate low values (Oehlert and Swart, 2014).
339 These circumstances make the Rumba low particularly interesting for further explorations of
340 depositional depth, diagenesis and the mix of isotopic signatures.

341 Other major negative $\delta^{13}\text{C}$ excursions in the Phanerozoic are associated with mass
342 extinctions (e.g. Schoene et al., 2010; Schulte et al., 2010; Shen et al., 2011), but the latest
343 Aeronian–earliest Telychian on the contrary represented a time of dramatic diversification of
344 graptolites (e.g. in *Parapetalolithus*, *Glyptograptus*, the retiolitids, *Rastrites* and *Streptograptus*;
345 see e.g. Loydell, 1994; Loydell et al., 2015), which makes the Rumba low all the more
346 intriguing. Clearly, the Rumba low warrants more detailed studies.

347 5.5 The Valgu positive excursion

348 The only manifestation of the Valgu excursion in the Sommerodde-1 core is from two
349 samples at 90.51 m and 89.62 m (Figure 6). At 90.51 m there is a positive shift of 1.2 ‰ by
350 comparison with the underlying sample at 91.69 m. This level is within the *Monoclimacis*
351 *griestoniensis* graptolite Biozone, which correlates with a level in the *Pterospathodus*
352 *eopennatus* ssp. n. 2 conodont Biozone (Loydell et al., 2003). In the Viki core, Estonia, peak
353 values of the Valgu excursion occur in the *P. eopennatus* ssp. n. 2 conodont Biozone (Munnecke
354 and Männick, 2009). Given that there is an excellent sedimentary and biostratigraphical record

355 through the lower and middle Telychian in the Sommerrodde-1 core, a sedimentary break seems
 356 unlikely to explain the lack of a more pronounced Valgu excursion. In the Viki core, the rising
 357 limb of the excursion occurs in the *P. eopennatus* ssp. n. 1 conodont Biozone. This conodont
 358 biozone correlates with the upper *Spirograptus turriculatus* and *Streptograptus crispus*
 359 graptolite biozones (Loydell et al., 1998; Loydell et al., 2003; Männik, 2007a; Walasek et al.,
 360 2018). In the *S. turriculatus* and *S. crispus* graptolite biozones in the Sommerrodde-1 core,
 361 however, the $\delta^{13}\text{C}_{\text{org}}$ values show only very minor fluctuations (Figure 6).

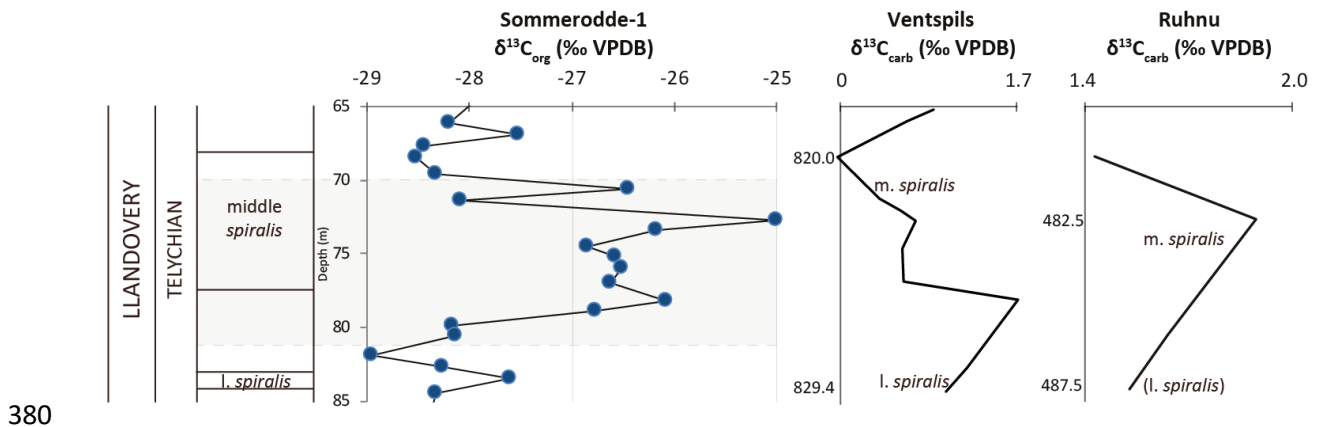


362
 363 Figure 6. The presumed Valgu positive carbon isotope excursion (grey field, dashed border) in the
 364 Sommerrodde-1 core (this study). Scale ranges from -27 to -39 ‰. In the Viki core, Estonia, the Valgu
 365 excursion is apparent in stratigraphically lower strata (Munnecke and Männick, 2009). For correlation
 366 between graptolite and conodont biozones, see Männik (2007b).

367 Since the Valgu excursion is not expressed in the $\delta^{13}\text{C}_{\text{org}}$ data despite the fact that
 368 deposition on southern Bornholm appears continuous through the interval, it emphasizes that
 369 we still do not understand why trends in $\delta^{13}\text{C}$ data are often, but not always, reflected in the
 370 records of both carbonate and organic carbon, or in shallow but not deep depositional settings.

371 5.6 The new Sommerodde positive isotope excursion (SOCIE)

372 The most pronounced positive excursion in the entire Upper Ordovician–Silurian of the
373 Sommerodde-1 core is seen between 80.55 m and 70.59 m, extending over several samples
374 within the *Oktavites spiralis* graptolite Biozone (Telychian) (Figure 7). In this interval, the
375 $\delta^{13}\text{C}_{\text{org}}$ values are significantly higher (-27.4 ‰) than on average for the entire succession (-
376 29.4 ‰ \pm 1.3) and the excursion has an amplitude of \sim 4 ‰. Peak values are higher (-25.4 ‰)
377 than those of both the HICE (-27.7 ‰) and the ESCIE (-27.1 ‰). Most of the excursion (77.02
378 m to 70.59 m) is demonstrably within the middle part of the *O. spiralis* Biozone (Loydell et al.,
379 2017). We name this new excursion the Sommerodde Carbon Isotope Excursion (SOCIE).



381 Figure 7. The positive Sommerodde carbon isotope excursion (SOCIE), newly recognized here, in the
382 *Oktavites spiralis* Biozone. Scale ranges from -25 to -30 ‰. Indications of a positive excursion may be
383 discerned in $\delta^{13}\text{C}_{\text{carb}}$ data from the Ventspils core in Latvia (Kaljo et al., 1998), and the Ruhnu core in
384 Estonia (Martma in Pöldvere, 2003); see also text below and Table 1 for references. The correlations
385 are based on intervals (Sommerodde-1) or levels (Ventspils and Ruhnu) with known biostratigraphical
386 data for the lower (l.), the middle (m.), and the upper (u.) *spiralis* Biozone ages. In the Ruhnu core, the
387 lower *spiralis* is assigned by the authors (Kaljo et al., 1998).

388 The discovery of SOCIE is a surprise considering that compilations of $\delta^{13}\text{C}$ data for the
389 Silurian (e.g. Cramer et al., 2011; Melchin et al., 2012; Sullivan et al., 2018) indicate that the
390 late Llandovery is characterized by a single negative excursion close to the base of the

391 Telychian, the Rumba low (see above), and a minor positive excursion, the Valgu excursion
392 (Munnecke and Männick, 2009), in the early–mid Telychian. The remainder of the Telychian
393 is shown as isotopically bland. Thus, the recognition of a second and quite distinct positive
394 excursion within the Telychian highlights the need for great caution when identifying
395 excursions in biostratigraphically poorly constrained sections.

396 The SOCIE can actually be discerned in previously published isotope curves from the
397 Baltic region. For example, the Ventspils D-3 core from Latvia shows a positive $\delta^{13}\text{C}_{\text{carb}}$
398 excursion of 2–3‰ within the 830–815 m interval (Kaljo et al., 1998, fig 5). The graptolite
399 biostratigraphy of this part of the core was investigated by Loydell and Nestor (2006) who
400 assigned assemblages from 826.7, 821.4 and 814.0 m to the lower, middle and upper *O. spiralis*
401 Biozone, respectively. The Ruhnu (500) core from Estonia also shows a small (<1‰) positive
402 excursion in $\delta^{13}\text{C}_{\text{carb}}$ at around 480 m (Martma in Pöldvere, 2003). Graptolites from 482.5 m
403 and 477.65 m in that core were assigned to the middle and upper *O. spiralis* Biozone,
404 respectively (Kaljo, in Pöldvere, 2003). The $\delta^{13}\text{C}_{\text{carb}}$ values decline through the lower part of
405 this interval and we infer that it reflects the declining limb of the SOCIE. In contrast, no positive
406 excursion is recognizable in the Viki core from Estonia, where post-Valgu excursion $\delta^{13}\text{C}_{\text{carb}}$
407 values exhibit only minor fluctuations and an overall gentle negative trend through most of the
408 Telychian (Kaljo et al., 2003). Other Baltic cores (e.g. Ikla; Gouldey et al., 2010) are
409 insufficiently densely sampled or lack sufficient biostratigraphical control to attempt
410 identification of the SOCIE.

411 The Baltic examples referred to above are all $\delta^{13}\text{C}_{\text{carb}}$ curves, which urges for a cautionary
412 comparison with the Sommerodde-1 $\delta^{13}\text{C}_{\text{org}}$ data. However, since all of the main Silurian
413 excursions discerned so far can be recognized in both $\delta^{13}\text{C}_{\text{carb}}$ and $\delta^{13}\text{C}_{\text{org}}$ records (e.g. Cramer
414 et al., 2011; Melchin and Holmden, 2006; Sullivan et al., 2018), an attempt to identify the
415 SOCIE in published $\delta^{13}\text{C}_{\text{carb}}$ curves is justifiable. In the four $\delta^{13}\text{C}_{\text{carb}}$ records discussed above

416 (the Ventspils D-3 core from Latvia and the Ruhnu (500), and Viki core from Estonia), the
417 SOCIE is not recognized in the shallowest setting (in the Viki core; Kaljo et al., 1998; Kaljo et
418 al., 2003). In contrast, the SOCIE is discernible in the Ventspils core, Latvia, which represents
419 the most paleo-offshore site of the four locations discussed. This pattern contrasts with other
420 records of Silurian positive excursions, where the magnitude declines basin-ward (Loydell
421 2007). Since mixing of isotopic fingerprints in particular is associated with early diagenesis in
422 shallow settings (Ahm et al., 2018; Fanton and Holmden, 2007; Higgins et al., 2018; Holmden
423 et al., 1998), an excursion in the deep Sommerodde-1 setting may serve as a reliable recording
424 of a global perturbation of the carbon cycle.

425 Outside the Baltic region, published $\delta^{13}\text{C}$ data from the Telychian are limited. Gouldey et
426 al. (2010) show a positive excursion within the Gettel Member of the Laketown Dolostone
427 Formation of the Pancake Range, Nevada, which is of assumed late Telychian age.
428 Unfortunately, the lack of biostratigraphical constraints hinders establishing precise age
429 brackets for this excursion. McAdams et al. (2017), in a study on the lower Silurian of Iowa,
430 show an un-zoned interval bracketed by occurrences of *Pt. am. angulatus* and *Pt. am.*
431 *amorphognathoides* (hence, including strata equivalent in age to the *O. spiralis* Biozone) to
432 exhibit only minor $\delta^{13}\text{C}_{\text{carb}}$ fluctuations and the SOCIE is not identifiable.

433 Taken together, the newly recognized SOCIE is intriguing in being a distinct positive
434 excursion that has not been widely recognized, and does not seem discernible in the shallow
435 settings in the Baltic basin. The SOCIE appears a suitable candidate for recording perturbations
436 in the global, open-marine setting.

437 5.7 The early Sheinwoodian carbon isotope excursion (ESCIE)

438 In the early Sheinwoodian, the Sommerodde-1 core data demonstrate a positive excursion
439 of $\sim 2\text{‰}$ that commences between 41.6 m (-28.87‰) and 40.05 m (-28.07‰) (Figure 2). At

440 41.05 m, *Mediograptus remotus* occurs and, at 39.67 m, *Euroclimacis adunca* occurs (Loydell
441 et al., 2017). While both taxa are typical of the *Cyrtograptus purchisoni* Biozone, *Me. remotus*
442 is restricted to the upper part of the biozone whilst *E. adunca* ranges into the overlying
443 *Monograptus firmus* Biozone (Štorch, 1994b). The biostratigraphical data are thus consistent
444 with the excursion commencing in the upper *C. purchisoni* Biozone (noting that the
445 immediately overlying strata are biostratigraphically undated). It is in the upper *C. purchisoni*
446 Biozone that the early Sheinwoodian positive carbon isotope excursion (ESCIE, sometimes
447 referred to as the Ireviken excursion, see discussion in Loydell 2007) has been observed to
448 commence elsewhere (e.g. Cramer et al., 2011; Lehnert et al., 2010; Loydell and Large, 2019).
449 The excursion ends between 32.02 m–31.30 m within strata containing undiagnostic graptolite
450 assemblages, dominated by *Pristiograptus dubius* and therefore assigned to the *Pristiograptus*
451 *dubius* Interval Zone, used by Štorch (1994b) and Zalasiewicz et al. (2009) for strata above the
452 LAD of *Monograptus riccartonensis* and below the FAD of the upper Sheinwoodian biozonal
453 indices *Cyrtograptus rigidus* and/or *Monograptus belophorus*.

454 The early Sheinwoodian positive carbon isotope excursion (ESCIE) has been the subject
455 of numerous studies, many of which are reviewed by Cramer et al. (2011) and Lehnert et al.
456 (2010). Since these reviews, the excursion has been identified also in the Barrandian area,
457 Czech Republic, by Frýda et al. (2015) and in Poland (e.g. Racki et al., 2012; Smolarek et al.,
458 2017; Sullivan et al., 2018), and a detailed study of the early stages of the excursion has been
459 undertaken on the Buttington section, Wales (Loydell and Large, 2019). In sections with good
460 biostratigraphical control, the ESCIE (with amplitudes varying from 2–4‰) can be seen to
461 begin high in the *Cyrtograptus purchisoni* Biozone (Loydell and Frýda, 2007, fig. 4; Loydell
462 and Large, 2019).

463 Overall, the stratigraphical position and amplitude of this excursion in the Sommerodde-1
464 core resemble those of the ESCIE as observed globally.

465 5.8 Still surprises in the Silurian

466 Our results demonstrate features in the Silurian $\delta^{13}\text{C}$ record that both add to and
 467 corroborate previous observations (see Table 1 for an overview).

468 **Table 1. Maximum amplitude (units of ‰) of the carbon isotope excursions discussed**

	Baltica						Laurentia					W	Gond.		Ya	Pe
	So	Bi	Es	La	Go	Po	CP	CM	NS	PR	DL		Li	Jo		
ESCIE	2		3 ¹		2 ²	4 ³						2 ⁴				4 ⁵
SOCIE	4		1 ⁶	3 ⁶						1 ⁷						
Valgu	1		2 ⁸													
Rumba (-)	10		3 ⁹							1 ⁷						
<i>Sedgwickii</i>	2							3 ¹⁰	4 ¹¹		3 ¹⁰					12 ¹²
EACIE	1		2 ⁹					1 ¹⁰			1 ¹⁰				1 ¹³	1 ¹⁴
mid-Rhudd.	1						2 ¹⁰				1 ¹⁵		2 ¹⁶	2 ¹⁷		
HICE	3	4 ¹⁸									6 ¹⁸					

469
 470 Carbon isotope excursions discussed here, as recognized on the continents of Baltica
 471 (Sommerodde-1 (So), Billegrav-2 (Bi), Estonia (Es), Latvia (La), Gotland (Go), Poland (Po)),
 472 Laurentia (Cape Phillips (CP), Cape Manning (CM), Nova Scotia (NS), Pancake Range (PR),
 473 Dob's Linn (Scotland)), Avalonia (Wales (W)), and Gondwana (Gond.; Libya (Li), Jordan (Jo))
 474 and on the Yangtze platform (Ya), and Perunica microcontinent (Pe). The studies are referred
 475 to in the text when discussing the carbon isotope excursion of the Hirnantian (HICE), the mid-
 476 Rhuddanian (mid-Rhud.), the early Aeronian (EACIE), the *Sedgwickii* Biozone, the Rumba low
 477 (Rumba; the only negative excursion), the Valgu, the Sommerodde (SOCIE), and the early
 478 Sheinwoodian (ESCIE). The $\delta^{13}\text{C}$ values are measured in organic carbon (bold) or carbonate
 479 (normal). Values from this study (So) and from (1) Loydell and Frýda 2007, (2) Munnecke et
 480 al., 2003, (3) Sullivan et al., 2018, (4) Loydell and Large 2019, (5) Frýda et al., 2015, (6) Kaljo
 481 et al, 1998, (7) Gouldey et al., 2010, (8) Munnecke and Männick 2009, (9) Kaljo and Martma
 482 2000, (10) Melchin and Holmden 2006, (11) Melchin et al., 2014, (12) Štorch and Frýda 2012,
 483 (13) Liu et al. 2017, (14) Štorch et al. 2018, (15) Underwood et al. 1997, (16) Loydell et al.,
 484 2013, (17) Loydell et al., 2009, (18) Hammarlund et al. 2012.

485 A surprise in this dataset, is the positive SOCIE excursion. The SOCIE, which spans over
 486 4 ‰, may previously have been recorded in $\delta^{13}\text{C}_{\text{carb}}$ data from palaeo-offshore cores in Estonia
 487 and Latvia, but not elsewhere. It is startling that the most significant excursion observed in the
 488 Sommerodde-1 core hitherto has remained unrecognized. Indeed, since processes in shallow
 489 settings appear to affect the amplification, alteration, and mixing of $\delta^{13}\text{C}$ trends (Fanton and
 490 Holmden, 2007; Higgins et al., 2018) an outboard setting with hemipelagic sedimentation that
 491 captures a significant positive isotope excursion may have particular value for understanding

492 global perturbations of the carbon cycle. Future studies of deep settings outside Baltica may
493 test whether SOCIE represents such a capture.

494 In contrast, the low $\delta^{13}\text{C}$ values in the Aeronian–Telychian boundary interval including
495 the Rumba low may represent an intriguing anomaly where, possibly, diagenesis has
496 overprinted the primary $\delta^{13}\text{C}$ values. For example, if the low isotope values are associated with
497 shallow depositional settings, the isotopic feature could have captured a local phenomenon
498 involving diagenesis. When early diagenesis of $\delta^{13}\text{C}_{\text{carb}}$ (and then $\delta^{13}\text{C}_{\text{org}}$) switches from being
499 buffered by open-marine fluids (deep) to being buffered by fluids from a restricted (shallow)
500 setting, the shift could be accompanied by specific and mixed isotopic signatures (Ahm et al.,
501 2018; Higgins et al., 2018). If the Rumba low has captured a mix of primary and diagenetic
502 carbon isotope signals, it provides an opportunity to decipher the two.

503 Taken together, both the Rumba low and the SOCIE appear tantalizing study intervals to
504 explore further. These events may provide clues to separate dynamics in the deep versus more
505 shallow settings. With geographically widespread evidence from these events, we can further
506 constrain how, when, and why global climate change occurred, affected, and directed the
507 evolution of animal life during the Ordovician and Silurian periods on Earth.

508 6 Conclusions

509 The Sommerodde-1 core from Bornholm, Denmark, provides a near-continuous
510 chemostratigraphical archive from the Upper Ordovician through to the Wenlock Series (lower
511 Silurian). A newly recognized positive carbon isotope excursion of $\sim 4\%$ in the Telychian
512 *Oktavites spiralis* Biozone (lower Silurian) is named the Sommerodde Carbon Isotope
513 Excursion (SOCIE). The SOCIE may be particularly valuable since the Sommerodde
514 depositional setting was comparatively deep, where the influence of diagenetic overprint or sea-
515 level change on the $\delta^{13}\text{C}_{\text{org}}$ signal was likely small. The Sommerodde-1 core section also reflects
516 previously recognized perturbations of the carbon cycle in the Hirnantian (HICE), the early

517 Aeronian (EACIE), the latest Aeronian-earliest Telychian (Rumba low), and the early
518 Sheinwoodian (ESCIE). Out of these observations, it is noteworthy that the EACIE commences
519 at the base of the *Demirastrites triangulatus* Biozone, as in the GSSP candidate Hlasná Třeboň
520 in the Czech Republic, suggesting it to be a useful chemostratigraphical marker. The absence
521 of an excursion in the *Spirograptus turriculatus* and *Streptograptus crispus* graptolite biozones
522 indicates a need to reassess the Valgu excursion.

523 Acknowledgements

524 We are grateful for the technical assistance from Dina Holmgaard Skov and Heidi Grøn
525 Jensen and to Tõnu Martma for sharing data. The study was part of a GeoCenter Denmark
526 projects [Grant 2015–5 and 2017–3]. We are grateful for the financial support from the Swedish
527 Research Council [Grant 2015-04693] and for the financial, technical, and academic support
528 from NordCEE and Don Canfield. We thank Dimitri Kaljo, Mike Melchin, Christian
529 Rasmussen, and Thomas Algeo for their constructive reviews.

530 References

- 531 Ahm, A.-S.C., Bjerrum, C.J., Blättler, C.L., Swart, P.K. and Higgins, J.A., 2018. Quantifying early marine
532 diagenesis in shallow-water carbonate sediments. *Geochimica et Cosmochimica Acta*, 236:
533 140-159.
- 534 Ahm, A.-S.C., Bjerrum, C.J. and Hammarlund, E.U., 2017. Disentangling the record of diagenesis, local
535 redox conditions, and global seawater chemistry during the latest Ordovician glaciation. *Earth
536 and Planetary Science Letters*, 459: 145-156.
- 537 Armstrong, H.A., Abbott, G.D., Turner, B.R., Makhlof, I.M., Muhammad, A.B., Pedentchouk, N. and
538 Peters, H., 2009. Black shale deposition in an Upper Ordovician–Silurian permanently
539 stratified, peri-glacial basin, southern Jordan. *Palaeogeography, Palaeoclimatology,
540 Palaeoecology*: 368–377.
- 541 Armstrong, H.A., Turner, B.R., Makhlof, I.M., Weedon, G.P., Williams, M., Al Smadi, A. and Abu Salah,
542 A., 2005. Origin, sequence stratigraphy and depositional environment of an Upper Ordovician
543 (Hirnantian) deglacial black shale, Jordan. *Palaeogeography, Palaeoclimatology,
544 Palaeoecology*, 220: 273–289.
- 545 Bjerreskov, M., 1975. Llandoveryan and Wenlockian graptolites from Bornholm. *Fossils and Strata*, 8.
- 546 Bjerreskov, M. and Jørgensen, K.Å., 1983. Late Wenlock graptolitebearing tuffaceous sandstone from
547 Bornholm, Denmark. *Bulletin of the Geological Society of Denmark*, 31: 129-149.
- 548 Calner, M., 2008. Silurian global events – at the tipping point of climate change, Mass Extinction.
549 Springer Berlin Heidelberg, pp. 21-57.

550 Calner, M., Ahlberg, P., Lehnert, O. and Erlström, M., 2013. The Lower Palaeozoic of southern Sweden
551 and the Oslo Region, Norway; Field Guide. In: M. Calner, P. Ahlberg, O. Lehnert and M. Erlström
552 (Editors), 3rd Annual Meeting of the IGCP project 591. SGU, Lund.

553 Cramer, B.D., Brett, C.E., Melchin, M.J., Männik, P., Kleffner, M.A., McLaughlin, P.I., Loydell, D.K.,
554 Munnecke, A., Jeppsson, L., Corradini, C., Brunton, F.R. and Saltzman, M.R., 2011. Revised
555 correlation of Silurian Provincial Series of North America with global and regional
556 chronostratigraphic units and $\delta^{13}\text{C}_{\text{carb}}$ chemostratigraphy. *Lethaia*, 44(2): 185-202.

557 Díaz-Martínez, E. and Grahn, Y., 2007. Early Silurian glaciation along the western margin of Gondwana
558 (Peru, Bolivia and northern Argentina): Palaeogeographic and geodynamic setting.
559 *Palaeogeography Palaeoclimatology Palaeoecology*, 245(1-2): 62-81.

560 Fanton, K.C. and Holmden, C., 2007. Sea-level forcing of carbon isotope excursions in epeiric seas:
561 implications for chemostratigraphy. *Canadian Journal of Earth Sciences*, 44(6): 807-818.

562 Frýda, J., Lehnert, O. and Joachimski, M., 2015. First record of the early Sheinwoodian carbon isotope
563 excursion (ESCIE) from the Barrandian area of northwestern peri-Gondwana. *Estonian Journal
564 of Earth Sciences*, 64: 42–46.

565 Gouldey, J.C., Saltzman, M.R., Young, S.A. and Kaljo, D., 2010. Strontium and carbon isotope
566 stratigraphy of the Llandovery (Early Silurian): implications for tectonics and weathering.
567 *Palaeogeography, Palaeoclimatology, Palaeoecology*, 296: 264–275.

568 Hammarlund, E.U., Dahl, T.W., Harper, D.A.T., Bond, D.P.G., Nielsen, A.T., Bjerrum, C.J., Schovsbo, N.H.,
569 Schönlaub, H.P., Zalasiewicz, J.A. and Canfield, D.E., 2012. A sulfidic driver for the end-
570 Ordovician mass extinction. *Earth and Planetary Science Letters*, 331-332C(0): 128-139.

571 Harper, D.A.T., Hammarlund, E.U. and Rasmussen, C.M.Ø., 2014. End Ordovician extinctions: A
572 coincidence of causes. *Gondwana Research*, 25(4): 1294-1307.

573 Heath, R.J., 1998. *Palaeoceanographic and Faunal Changes in the Early Silurian*, University of Liverpool,
574 Liverpool, 239 pp.

575 Higgins, J.A., Blättler, C.L., Lundstrom, E.A., Santiago-Ramos, D.P., Akhtar, A.A., Crüger Ahm, A.S., Bialik,
576 O., Holmden, C., Bradbury, H., Murray, S.T. and Swart, P.K., 2018. Mineralogy, early marine
577 diagenesis, and the chemistry of shallow-water carbonate sediments. *Geochimica et
578 Cosmochimica Acta*, 220: 512-534.

579 Holmden, C., Creaser, R.A., Muehlenbachs, K., Leslie, S.A. and Bergström, S.M., 1998. Isotopic evidence
580 for geochemical decoupling between ancient epeiric seas and bordering oceans: Implications
581 for secular curves. *Geology*, 26(6): 567-570.

582 Kaljo, D., Kiipli, T. and Martma, T., 1998. Correlation of carbon isotope events and environmental
583 cyclicity in the East Baltic Silurian. *New York State Museum Bulletin*, 491: 297–327.

584 Kaljo, D. and Martma, T., 2000. Carbon isotopic composition of Llandovery rocks (East Baltic Silurian)
585 with environmental interpretation. *Proceedings of the Estonian Academy of Sciences, Geology*
586 49: 267–283.

587 Kaljo, D., Martma, T., Männik, P. and Viira, V., 2003. Implications of Gondwana glaciations in the Baltic
588 late Ordovician and Silurian and a carbon isotopic test of environmental cyclicity. *Bulletin de
589 la Société Géologique de France*, 174: 59–66.

590 Kaljo, D. and Vingisaar, P., 1969. On the sequence of the Raikküla Stage in southernmost Estonia. *Eesti
591 NSV Teadvste Akadeemia, Toimetised, Keemia Geoloogi*, 18: 270–277.

592 Koren', T. and Bjerreskov, M., 1997. Early Llandovery monograptids from Bornholm and the southern
593 Urals: taxonomy and evolution. *Bulletin of the Geological Society of Denmark*, 44: 1-43.

594 Lehnert, O., Männik, P., Joachimski, M.M., Calner, M. and Frýda, J., 2010. Palaeoclimate perturbations
595 before the Sheinwoodian glaciation: a trigger for extinctions during the 'Ireviken Event'.
596 *Palaeogeography, Palaeoclimatology, Palaeoecology* 296: 320–331.

597 Liu, Z., Algeo, T.J., Guo, X., Fan, J., Du, X. and Lu, Y., 2017. Paleo-environmental cyclicity in the Early
598 Silurian Yangtze Sea (South China): tectonic or glacio-eustatic control? . *Palaeogeography,
599 Palaeoclimatology, Palaeoecology*, 466: 59–76.

600 Loydell, D.K., 1994. Early Telychian changes in graptoloid diversity and sea level. *Geological Journal*,
601 29: 355–368.

602 Loydell, D.K., 1998. Early Silurian sea-level changes. *Geological Magazine*, 135(4): 447-471.

603 Loydell, D.K., 2007. Early Silurian positive $\delta^{13}\text{C}$ excursions and their relationship to glaciations, sea-
604 level changes and extinction events. *Geological Journal*, 42(5): 531-546.

605 Loydell, D.K., 2012. Graptolite biostratigraphy of the E1-NC174 core, Rhuddanian (lower Llandovery,
606 Silurian), Murzuq Basin (Libya). *Bulletin of Geosciences*, 87: 651–660.

607 Loydell, D.K., Butcher, A. and Frýda, J., 2013. The middle Rhuddanian (lower Silurian) ‘hot’ shale of
608 North Africa and Arabia: An atypical hydrocarbon source rock. *Palaeogeography,*
609 *Palaeoclimatology, Palaeoecology*, 386: 233-256.

610 Loydell, D.K., Butcher, A., Frýda, J., Lüning, S. and Fowler, M., 2009. Lower Silurian “hot shales” in
611 Jordan: a new depositional model. *Journal of Petroleum Geology*, 32: 261–270.

612 Loydell, D.K. and Frýda, J., 2007. Carbon isotope stratigraphy of the upper Telychian and lower
613 Sheinwoodian (Llandovery–Wenlock, Silurian) of the Banwy River section, Wales. *Geological*
614 *Magazine* 144: 1015–1019.

615 Loydell, D.K., Frýda, J. and Gutiérrez-Marco, J.C., 2015. The Aeronian/Telychian (Llandovery, Silurian)
616 boundary, with particular reference to sections around the El Pintado reservoir, Seville
617 Province, Spain. *Bulletin of Geosciences*, 90: 743–794.

618 Loydell, D.K., Kaljo, D. and Männik, P., 1998. Integrated biostratigraphy of the lower Silurian of the
619 Ohesaare core, Saaremaa, Estonia. *Geological Magazine* 135: 769–783.

620 Loydell, D.K. and Large, R.R., 2019. Biotic, geochemical and environmental changes through the early
621 Sheinwoodian (Wenlock, Silurian) carbon isotope excursion (ESCIE), Buttington Quarry, Wales.
622 *Palaeogeography, Palaeoclimatology, Palaeoecology*, 514: 305-325.

623 Loydell, D.K., Maletz, J. and Nestor, V., 2003. Integrated biostratigraphy of the lower Silurian of the
624 Aizpute-41 core, Latvia. *Geological Magazine*, 140: 205–229.

625 Loydell, D.K. and Nestor, V., 2006. Isolated graptolites from the Telychian (upper Llandovery) of Latvia
626 and Estonia. *Palaeontology* 49: 585–619.

627 Loydell, D.K., Nestor, V. and Maletz, J., 2010. Integrated biostratigraphy of the lower Silurian of the
628 Kolka-54 core, Latvia. *Geological Magazine*, 147: 253–280.

629 Loydell, D.K., Walasek, N., Schovsbo, N.H. and Nielsen, A.T., 2017. Graptolite biostratigraphy of the
630 lower Silurian of the Sommerodde-1 core, Bornholm, Denmark. *Bulletin of the Geological*
631 *Society of Denmark*, 65: 135-160.

632 Maletz, J., 1997. Ordovician and Silurian strata of the G-14 well (Baltic Sea): graptolite faunas and
633 biostratigraphy. *Zeitschrift für Geologische Wissenschaften*, 25: 29-39.

634 McAdams, N.E.B., Bancroft, A.M., Cramer, B.D. and Witzke, B.J., 2017. Integrated carbon isotope and
635 conodont biochemostratigraphy of the Silurian (Aeronian–Telychian) of the east-central Iowa
636 Basin, Iowa, USA. *Newsletters on Stratigraphy*, 50: 391–416.

637 Melchin, M.J. and Holmden, C., 2006. Carbon isotope chemostratigraphy of the Llandovery in Arctic
638 Canada: implications for global correlation and sea-level change. *GFF*, 128: 173–180.

639 Melchin, M.J., MacRae, K.-D. and Bullock, P., 2014. A multi-peak organic carbon isotope excursion in
640 the late Aeronian (Llandovery, Silurian): evidence from Arisaig, Nova Scotia, Canada.
641 *Palaeoworld*, 24: 191–197.

642 Melchin, M.J., Sadler, P.M. and Cramer, B.D., 2012. The Silurian Period. In: F.M. Gradstein, J.G. Ogg,
643 M.D. Schmitz and G.M. Ogg (Editors), *The geologic time scale 2012*. Elsevier, Amsterdam, pp.
644 525–558.

645 Munnecke, A. and Männik, P., 2009. New biostratigraphic and chemostratigraphic data from the
646 Chicotte Formation (Llandovery, Anticosti Island, Laurentia) compared with the Viki core
647 (Estonia, Baltica). *Estonian Journal of Earth Sciences*, 58: 159–169.

648 Männik, P., 2007a. Some comments on Telychian–early Sheinwoodian conodont faunas, events and
649 stratigraphy. *Acta Palaeontologica Sinica*, 46: 305–310.

650 Männik, P., 2007b. An updated Telychian (Late Llandovery, Silurian) conodont zonation based on Baltic
651 faunas. *Lethaia*, 40: 45–60.

652 Nielsen, A.T., 2004. Sea-level Changes - a Baltoscandian Perspective. In: B.D. Webby, M.L. Droser, F.
653 Paris and I.G. Percival (Editors), *The Great Ordovician Biodiversification Event, Part II.*
654 *Conspectus of the Ordovician World*, Columbia pp. 84-93.

655 Oehlert, A.M. and Swart, P.K., 2014. Interpreting carbonate and organic carbon isotope covariance in
656 the sedimentary record. *Nature Communications*, 5: 4672.

657 Petersen, H.I., Schovsbo, N.H. and Nielsen, A.T., 2013. Reflectance measurements of zooclasts and
658 solid bitumen in Lower Paleozoic shales, southern Scandinavia: Correlation to vitrinite
659 reflectance. *International Journal of Coal Geology*, 114: 1-18.

660 Põldvere, A., 2003. Ruhnu (500) drill core. *Estonian Geological Sections Bulletin*, 5: 1–38.

661 Racki, G., Baliński, A., Wrona, R., Małkowski, K., Drygany, D. and Szaniawski, H., 2012. Faunal dynamics
662 across the Silurian–Devonian positive isotope excursions (613C, 618O) in Podolia, Ukraine:
663 comparative analysis of the Ireviken and Klonk events. *Acta Palaeontologica Polonica*, 57: 795–
664 832.

665 Schoene, B., Guex, J., Bartolini, A., Schaltegger, U. and Blackburn, T.J., 2010. Correlating the end-
666 Triassic mass extinction and flood basalt volcanism at the 100 ka level. *Geology* 38: 387–390.

667 Schovsbo, N.H., A.T., N. and Klitten, K., 2015. The Lower Palaeozoic now fully cored and logged on
668 Bornholm. *Geological Survey of Denmark and Greenland Bulletin*, 33: 9-12.

669 Schovsbo, N.H., Nielsen, A.T. and Erlström, M., 2016. Middle–Upper Ordovician and Silurian
670 stratigraphy and basin development in southernmost Scandinavia. *Geological Survey of*
671 *Denmark and Greenland Bulletin*, 35: 39–42.

672 Schulte, P., Alegret, L., Arenillas, I., Arz, J.A., Barton, P.J., Bown, P.R., Bralower, T.J., Christeson, G.L.,
673 Claeys, P., Cockell, C.S., Collins, G.S., Deutsch, A., Goldin, T.J., Goto, K., Grajales-Nishimura,
674 J.M., Grieve, R.A.F., Gulick, S.P.S., Johnson, K.R., Kiessling, W., Koeberl, C., Kring, D.A.,
675 MacLeod, K.G., Matsui, T., Melosh, J., Montanari, A., Morgan, J.V., Neal, C.R., Nichols, D.J.,
676 Norris, R.D., Pierazzo, E., Ravizza, G., Rebolledo-Vieyra, M., Reimold, W.U., Robin, E., Salge, T.,
677 Speijer, R.P., Sweet, A.R., Urrutia-Fucugauchi, J., Vajda, V., Whalen, M.T. and Willumsen, P.S.,
678 2010. The Chicxulub Asteroid Impact and Mass Extinction at the Cretaceous-Paleogene
679 Boundary. *Science*, 327(5970): 1214-1218.

680 Scotese, C.R., 2001. *Atlas of Earth History*, Arlington, Texas, pp. 52 Volume 1, Paleogeography,
681 PALEOMAP Project.

682 Servais, T., Harper, D.A.T., Munnecke, A., Owen, A.W. and Sheehan, P.M., 2009. Understanding the
683 great ordovician biodiversification event (GOBE): influences of paleogeography, paleoclimate,
684 or paleoecology. *GSA Today*, 4: 4-10.

685 Shen, S.-z., Crowley, J.L., Wang, Y., Bowring, S.A., Erwin, D.H., Sadler, P.M., Cao, C.-q., Rothman, D.H.,
686 Henderson, C.M., Ramezani, J., Zhang, H., Shen, Y., Wang, X.-d., Wang, W., Mu, L., Li, W.-z.,
687 Tang, Y.-g., Liu, X.-l., Liu, L.-j., Zeng, Y., Jiang, Y.-f. and Jin, Y.-g., 2011. Calibrating the End-
688 Permian Mass Extinction. *Science*, 334(6061): 1367-1372.

689 Smolarek, J., Trela, W., Bond, D.P.G. and Marynowski, L., 2017. Lower Wenlock black shales in the
690 northern Holy Cross Mountains, Poland: sedimentary and geochemical controls on the Ireviken
691 Event in a deep marine setting. *Geological Magazine*, 154: 247–264.

692 Štorch, P., 1994a. Graptolite biostratigraphy of the lower Silurian (Llandovery and Wenlock) of
693 Bohemia. *Geological Journal*, 29: 137–165.

694 Štorch, P., 1994b. Llandovery–Wenlock boundary beds in the graptolite-rich sequence of the
695 Barrandian area (Bohemia). *Journal of the Czech Geological Society*, 39: 163–182.

696 Štorch, P. and Frýda, J., 2012. The late Aeronian graptolite sedgwickii Event, associated positive carbon
697 isotope excursion and facies changes in the Prague Synform (Barrandian area, Bohemia).
698 *Geological Magazine*, 149: 1089–1106.

699 Štorch, P., Manda, Š., Tasáryová, Z., Frýda, J., Chadimová, L. and Melchin, M.J., 2018. A proposed new
700 global stratotype for Aeronian Stage of the Silurian System: Hlásná Třebaň section, Czech
701 Republic. *Lethaia* 51: 357–388.

- 702 Stouge, S., 2004. Ordovician siliciclastics and carbonates of Öland, Sweden. In: A. Munnecke, T. Servais
703 and C. Schulbert (Editors), International Symposium on Early Palaeozoic Palaeogeography and
704 Palaeoclimate. Erlanger geologische Abhandlungen, Erlangen, pp. 91–111.
- 705 Sullivan, N.B., Loydell, D.K., Montgomery, P., Molyneux, S., Zalasiewicz, J., Ratcliffe, K.T., Campbell, E.,
706 Griffiths, J.D. and Lewis, G., 2018. A record of Late Ordovician to Silurian oceanographic events
707 on the margin of Baltica based on new carbon isotope data, elemental geochemistry, and
708 biostratigraphy from two boreholes in central Poland. *Palaeogeography, Palaeoclimatology,
709 Palaeoecology*, 490: 95–106.
- 710 Underwood, C.J., Crowley, S.F., Marshall, J.D. and Brenchley, P.J., 1997. High-resolution carbon isotope
711 stratigraphy of the basal Silurian stratotype (Dob's Linn, Scotland) and its global correlation.
712 *Journal of the Geological Society*, 154: 709-718.
- 713 Walasek, N., Loydell, D.K., Frýda, J. and Loveridge, R.F., 2018. Integrated graptolite-conodont
714 biostratigraphy and organic carbon chemostratigraphy of the Llandovery of Kallholn quarry,
715 Dalarna, Sweden. *Palaeogeography, Palaeoclimatology, Palaeoecology*, 508: 1-16.
- 716 Veizer, J., 2005. Celestial climate driver: a perspective from four billion years of the carbon cycle.
717 *Geoscience Canada*, 32: 13-28.
- 718 Zalasiewicz, J.A., Taylor, L., Rushton, A.W.A., Loydell, D.K., Rickards, R.B. and Williams, M., 2009.
719 Graptolites in British stratigraphy. *Geological Magazine*, 146: 785–850.

720